# Which factors of an Active Region determine whether a flare will be CME-associated or not?

**Christian Baumgartner, Julia K. Thalmann, Astrid M. Veronig**

Institute of Physics & Kanzelhöhe Observatory, University of Graz, Austria

# Motivation

Intro

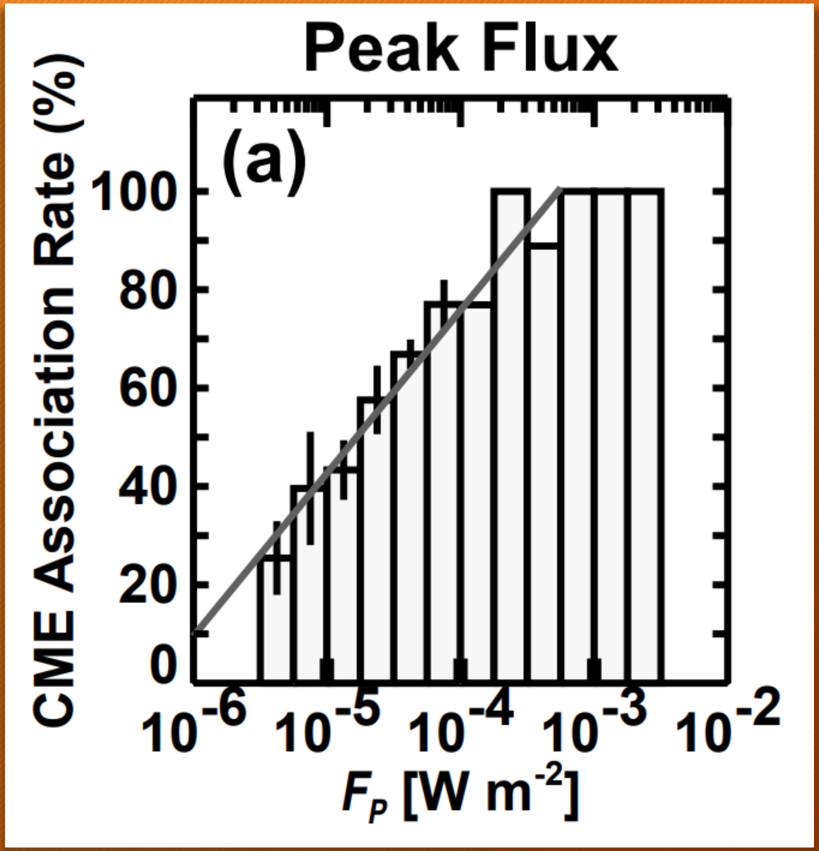


More energetic flares are more likely to be eruptive

X-Class Flares ($10^{-4}\ \mathrm{W\ m^{-2}}$ Peak SXR Flux)

$>90\%$ CME association rate

Yashiro et al. (2006)

# Motivation

Intro

Exceptions:

NOAA 12192 (17-30 October 2014)
Largest AR since 1990

- 6 X-class and 30 M-class flares
- only 1 M-class flare was eruptive!

(e.g. Thalmann et al. 2015, Sun et al. 2015)

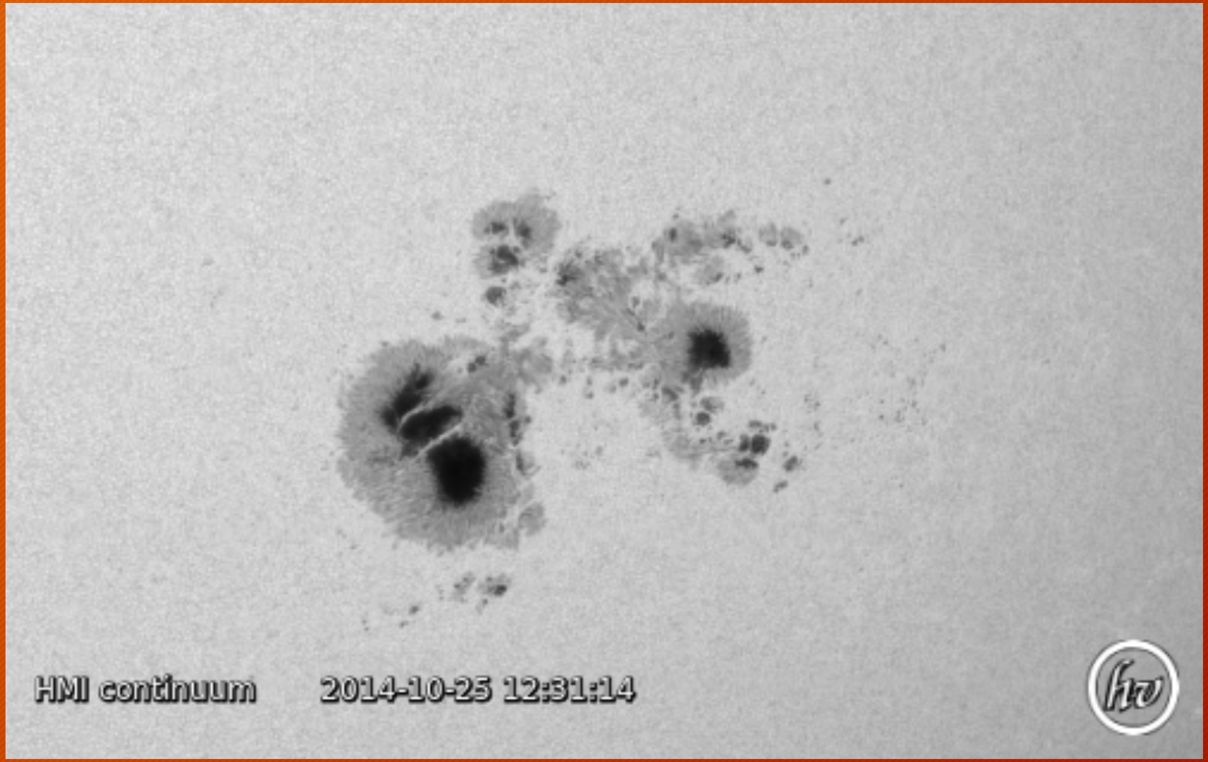

# Goal



- Better understanding of the role of the ARs magnetic structure in the production of large confined vs. eruptive flares

Approach: Investigate the

1) Flare location within the host active region
2) Magnetic field strength in the corona above the flaring region
3) Magnetic field orientation in the corona above the flaring region

# Event Selection

Study Setup

- Criteria:
  - GOES class $\geq$ M5.0 ("large" flares)
  - Flare location $\leq 50^\circ$ from the solar disk's center
  - January 2011 – December 2015
- 44 large flares
  - 12 confined (7 M- and 5 X-flares)
  - 32 eruptive (18 M- and 14 X-flares)

# Data and Methods

Study Setup

3D potential field models for each event:

- based on the Fourier transformation method (Alissandrakis, 1981)
- extrapolated from photospheric magnetic field observations using SDO/HMI data (Schou et al. 2012)
- at least 12 mins prior to the onset of the flare
- identification of flare-relevant regions using SDO/AIA data (Lemen et al. 2012)

# Extent of Host Active Region

**Method**

$d_{PC}$ … distance between opposite magnetic polarity centers (flux weighted centers)

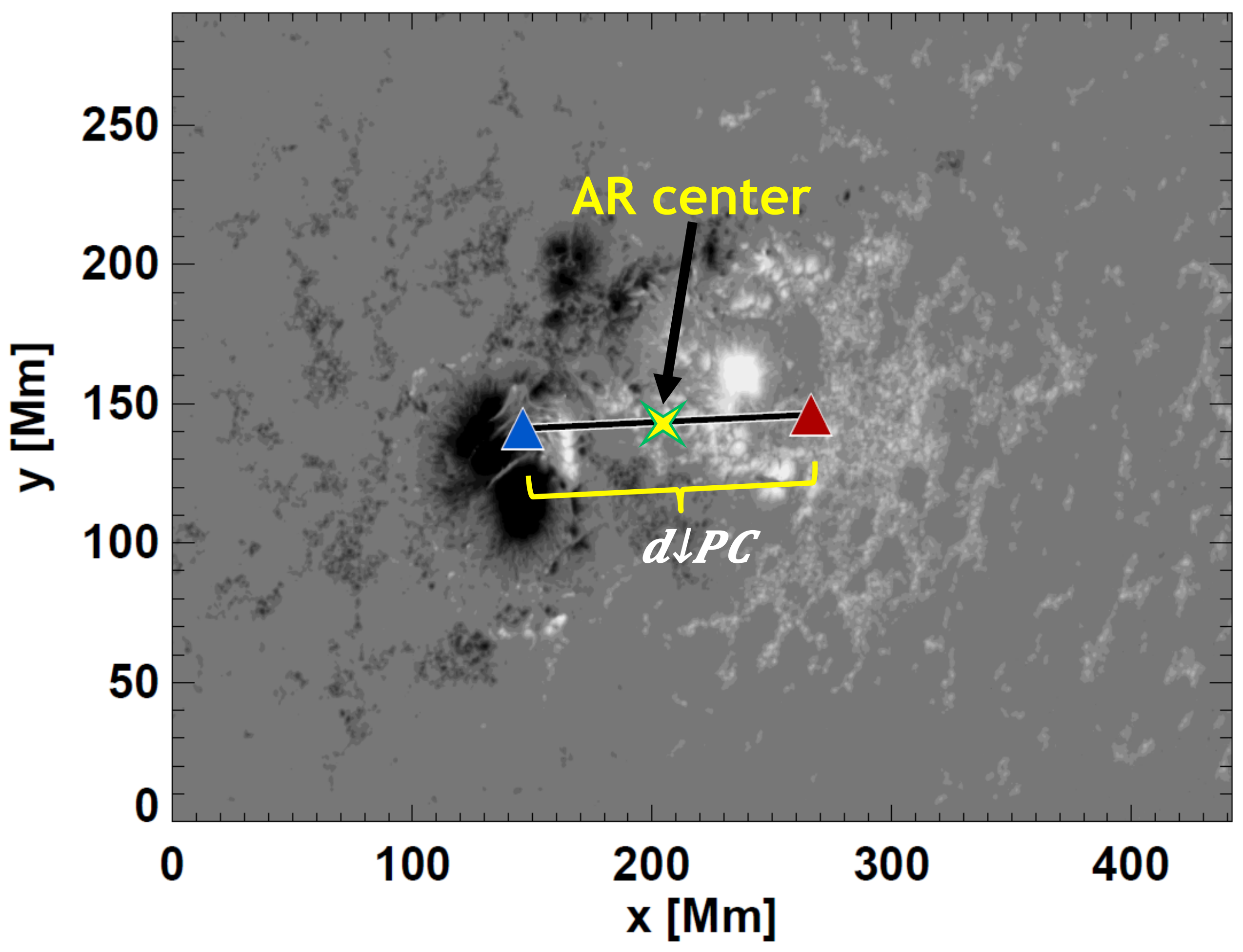


NOAA 12192 on October 25, 2014 (16:47 UT)

# Extent of Host Active Region

**Method**

$d_{PC}$ … distance between opposite magnetic polarity centers

→ ½ $d_{PC}$ approximates AR’s dipole radius!

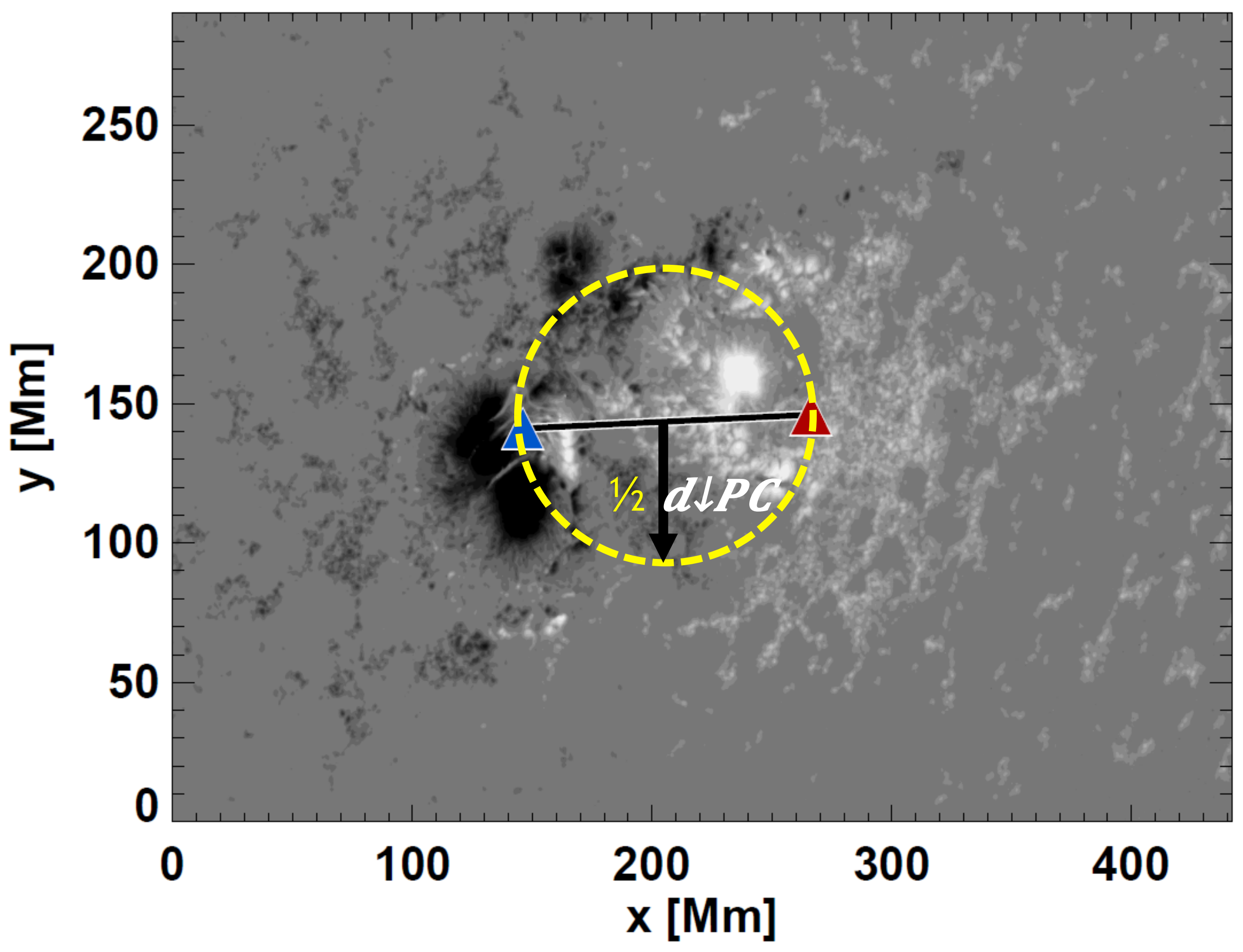


NOAA 12192 on October 25, 2014 (16:47 UT)

# Flare Location

Method

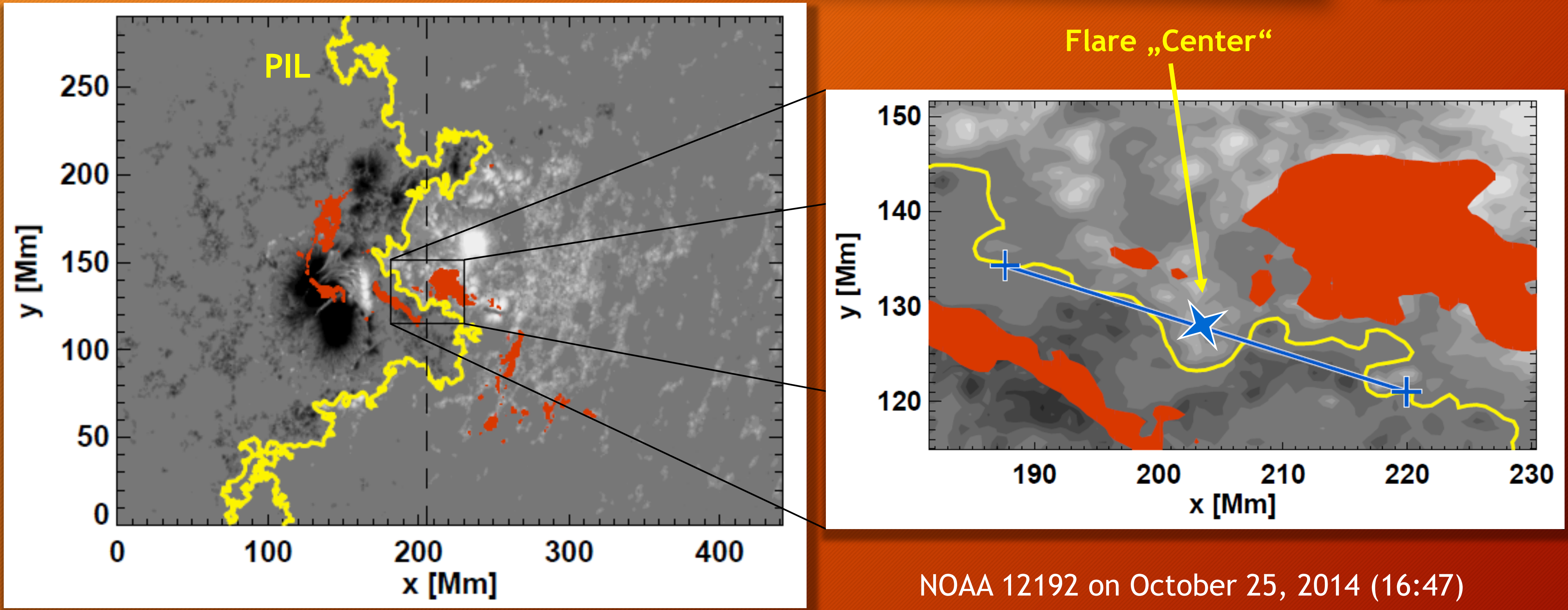


NOAA 12192 on October 25, 2014 (16:47)

# Flare Distance from Active-Region Center

Method

- $d_{FC}$ … distance between flare site and flux weighted AR center

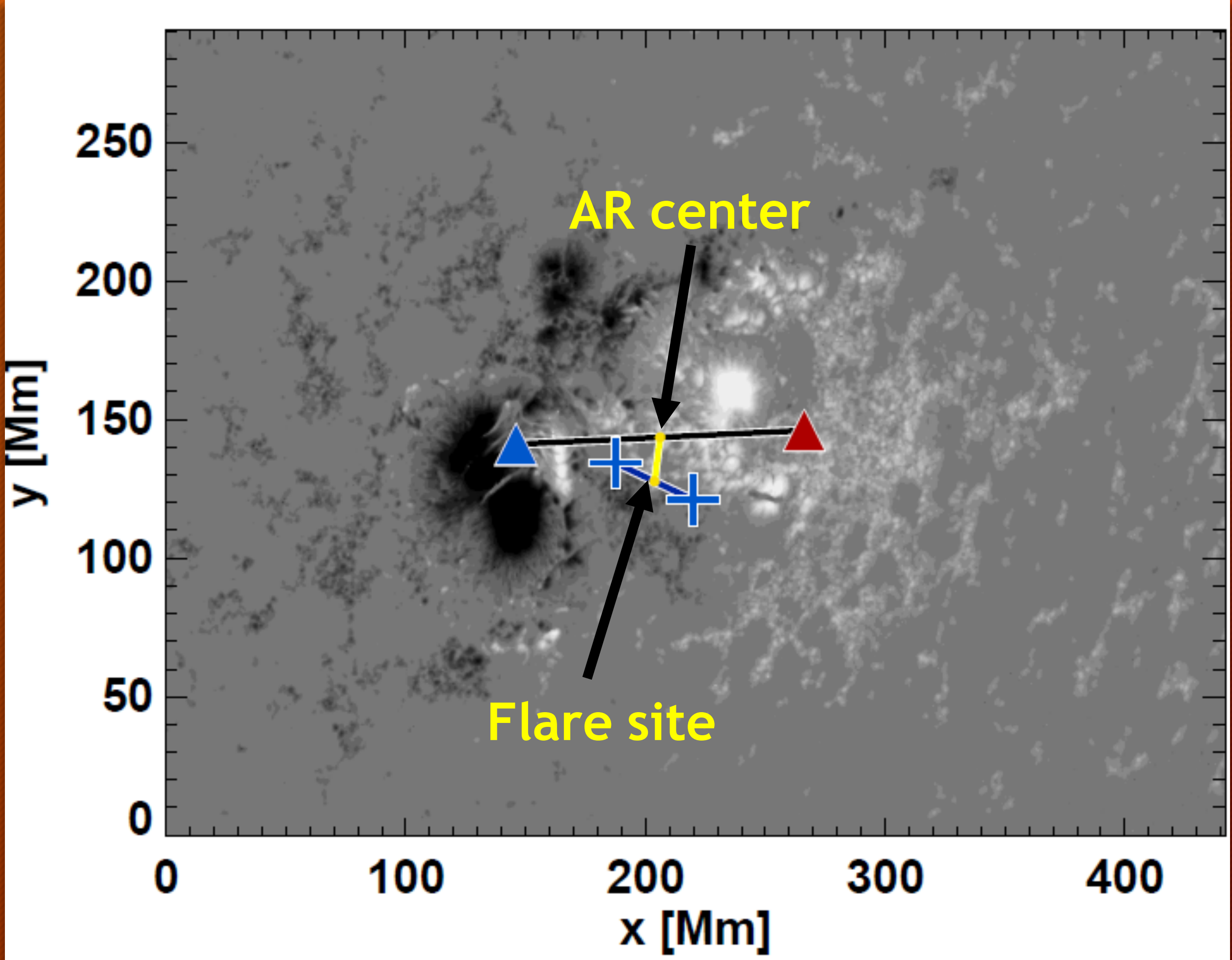


NOAA 12192 on October 25, 2014 (16:47)

# Flare Distance from Active-Region Center

Method

- $d_{FC}$ … distance between flare site and flux weighted AR center

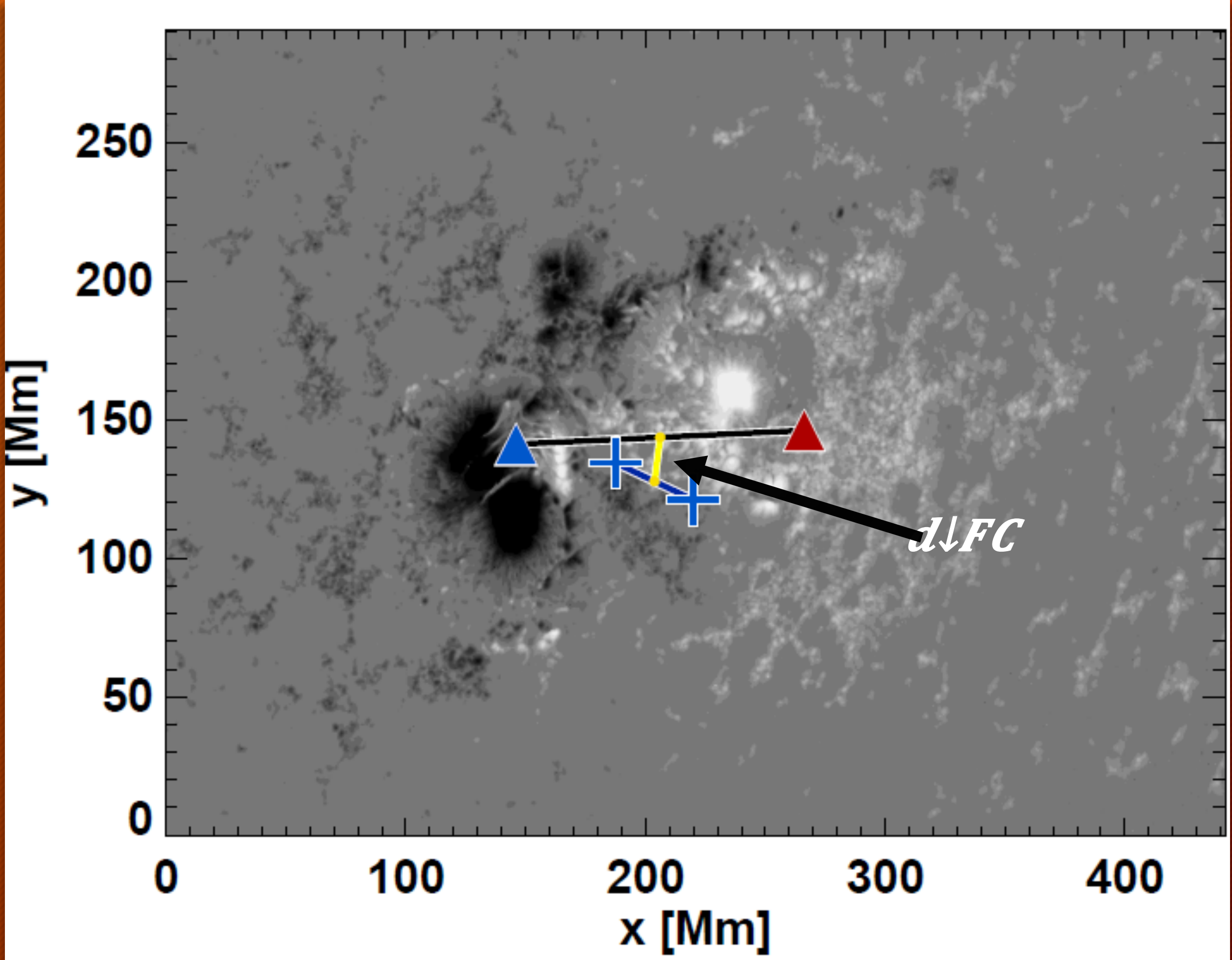


NOAA 12192 on October 25, 2014 (16:47)

# Relative Location of Flare Site within Host Active Region

Results

Flare distance from AR center normalized by the extent of the host's AR dipole $d_{FC} / d_{PC}$ against $d_{PC}$

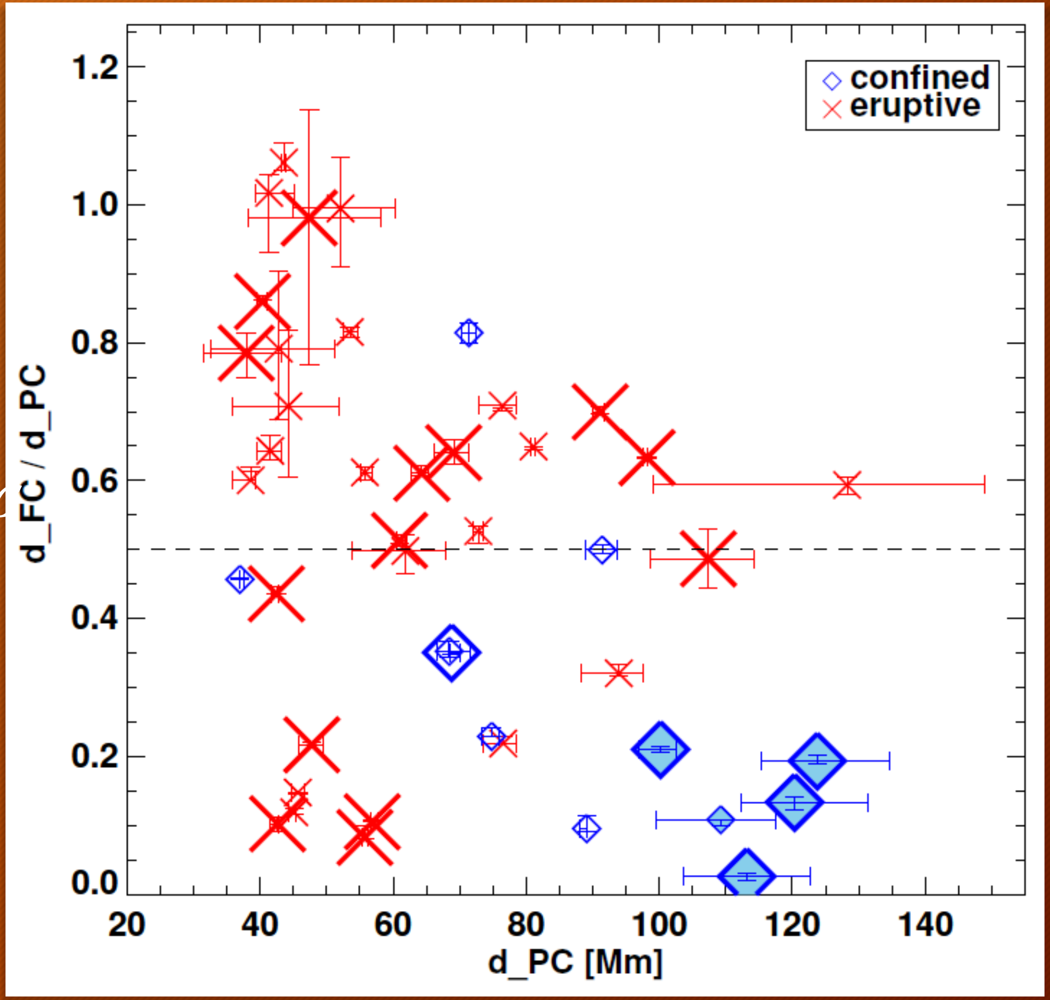

# Relative Location of Flare Site within Host Active Region

**Results**

Flare distance from AR center normalized by the extent of the host's AR dipole $d_{FC} / d_{PC}$ against $d_{PC}$

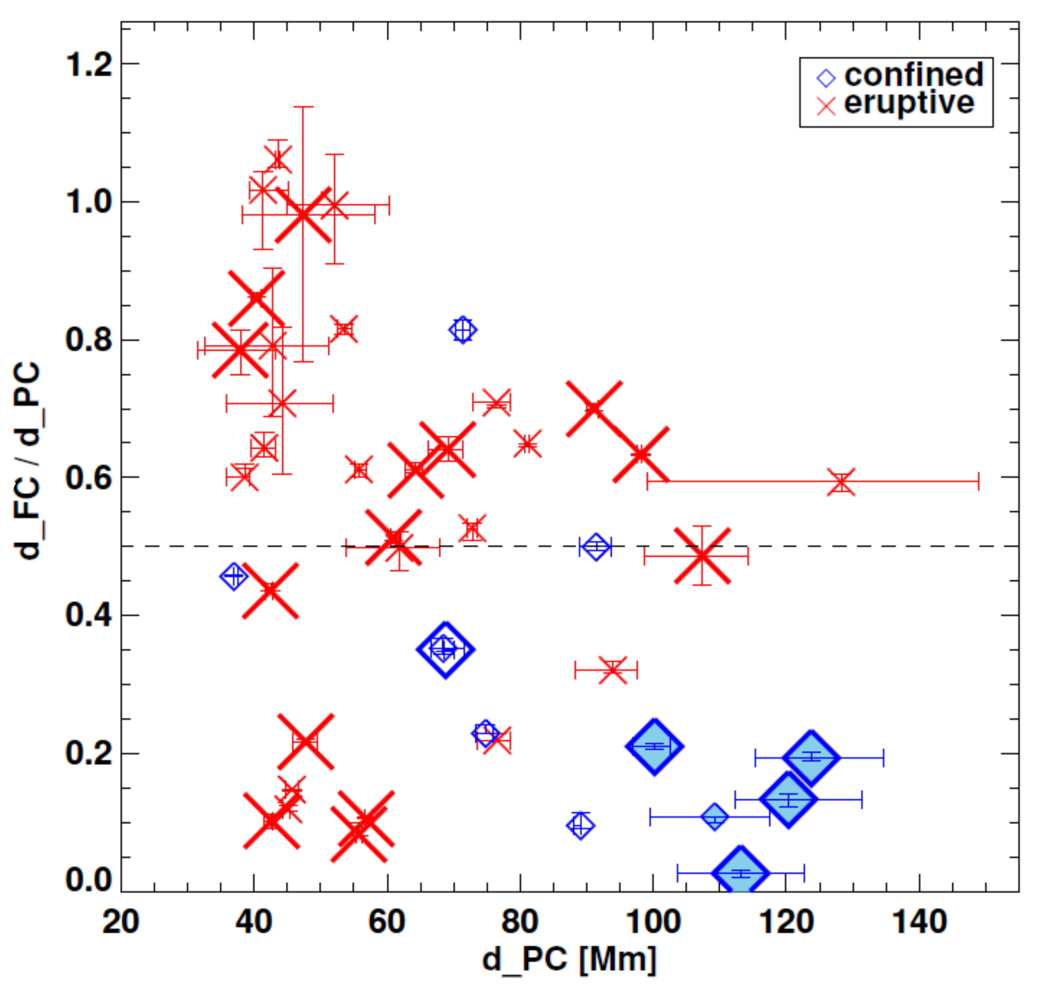


In periphery of the host AR's dipole field

Enclosed by AR dipole field

# Relative Location of Flare Site within Host Active Region

Results

Flare distance from AR center normalized by the extent of the host's AR dipole $d_{FC} / d_{PC}$ against $d_{PC}$

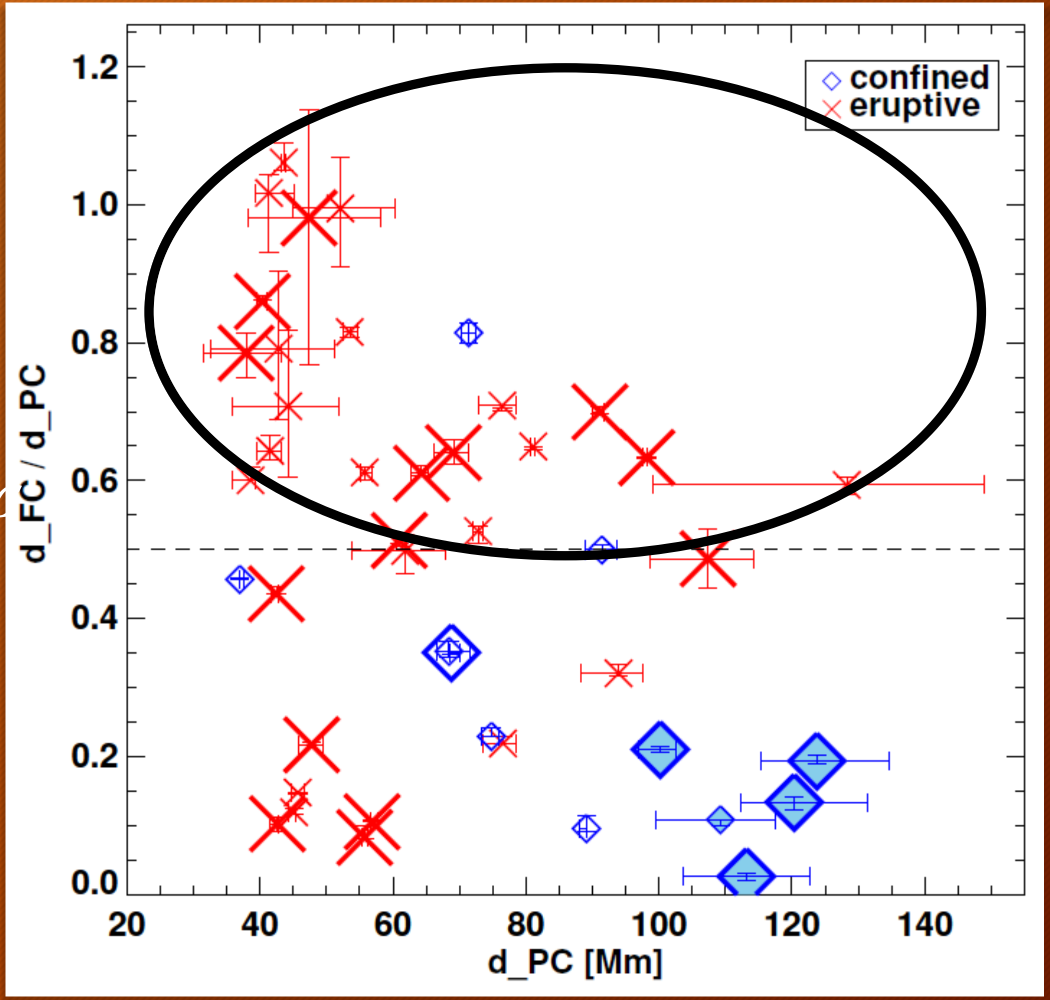


In periphery of the host AR's dipole field

Enclosed by AR dipole field

# Relative Location of Flare Site within Host Active Region

Results

Flare distance from AR center normalized by the extent of the host's AR dipole $d_{FC} / d_{PC}$ against $d_{PC}$

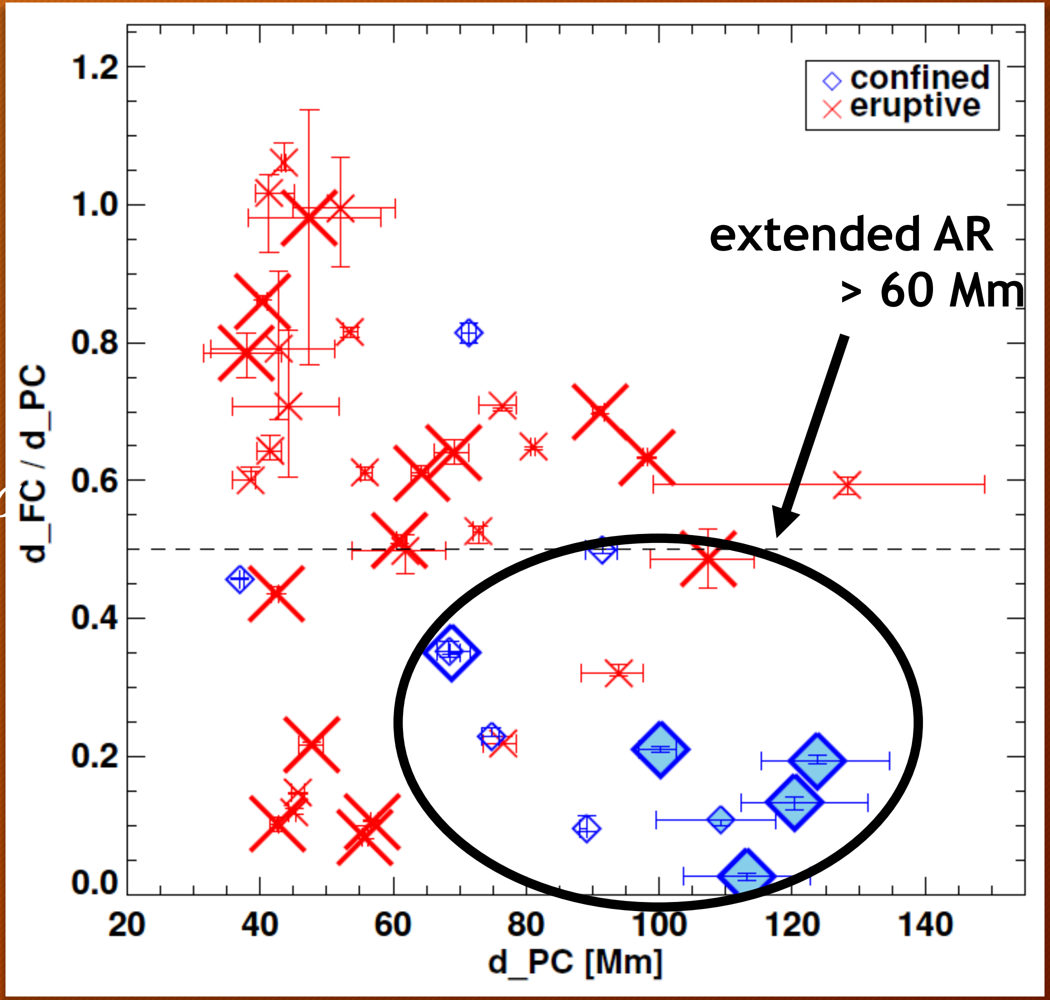


In periphery of the host AR's dipole field

Enclosed by AR dipole field

# Relative Location of Flare Site within Host Active Region

Results

Flare distance from AR center normalized by the extent of the host‘s AR dipole $d_{FC} / d_{PC}$ against $d_{PC}$

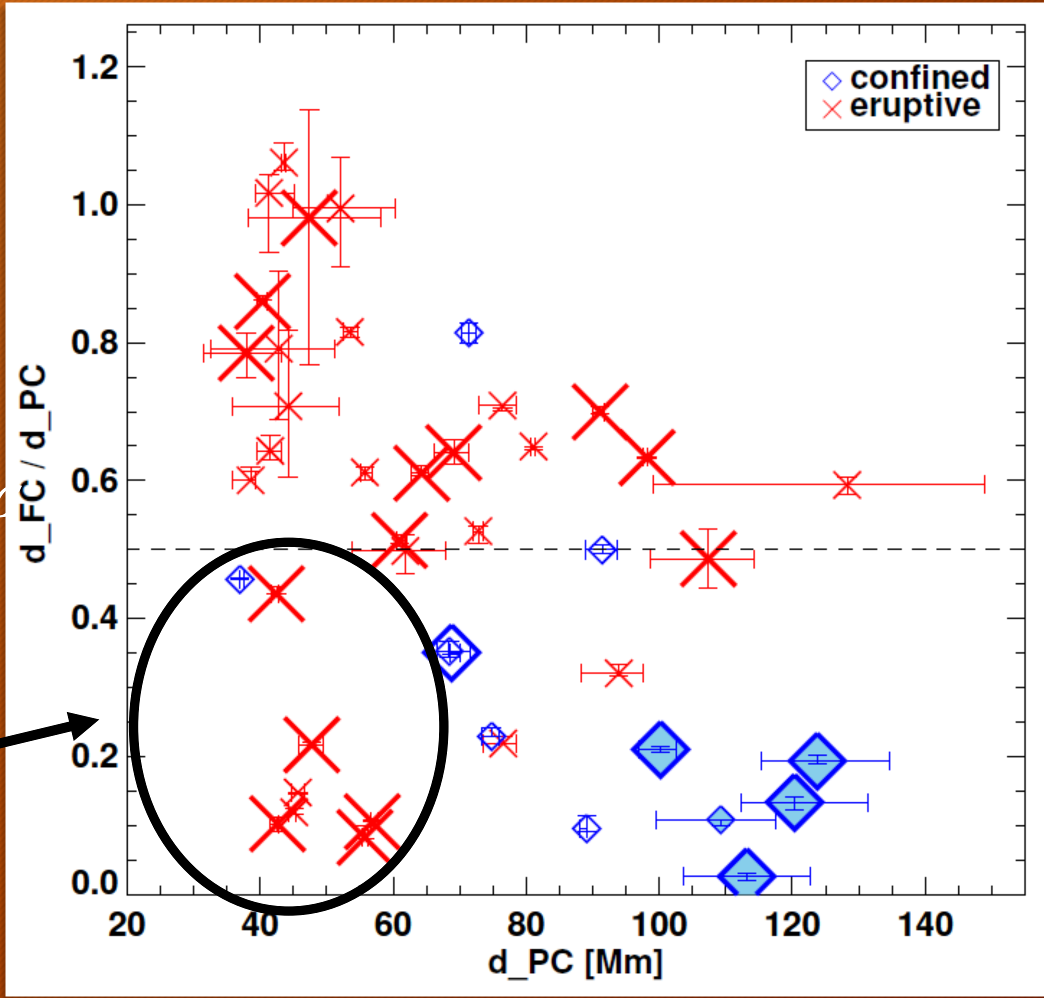


**compact AR**
**$d_{PC}$ < 60 Mm**

In periphery of the host AR‘s dipole field

Enclosed by AR dipole field

# Strength of Magnetic Field Above Flare Site

**Method**

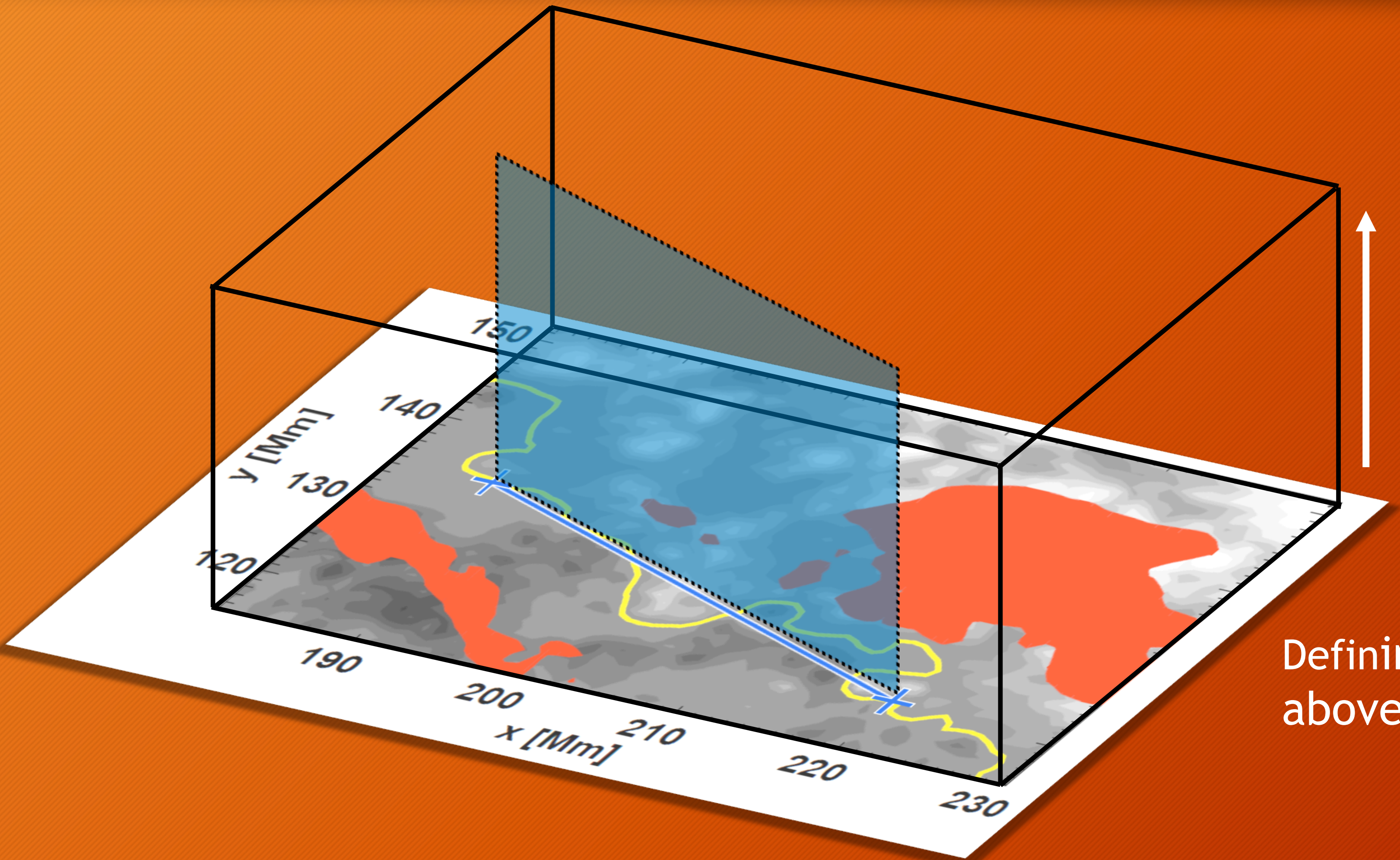


model height
above photosphere

Defining a vertical plane
above flare-relevant PIL

# Strength of Magnetic Field Above Flare Site

Method

Decay Index $n$ (Kliem & Török 2006)

$$n = -\frac{d \ln B_{hor}}{d \ln h}$$

$B_{hor}$ … horizontal field strength

$h$ … height in the corona

Critical height for torus instability of cylindrical fluxrope:

$$h_{crit} = h\left(\langle n \rangle \approx 1.5\right)$$

(Török & Kliem 2007, Fan & Gibson 2007, Démoulin & Aulanier 2010, Zuccarello et al. 2015)

# Strength of Magnetic Field Above Flare Site

Method

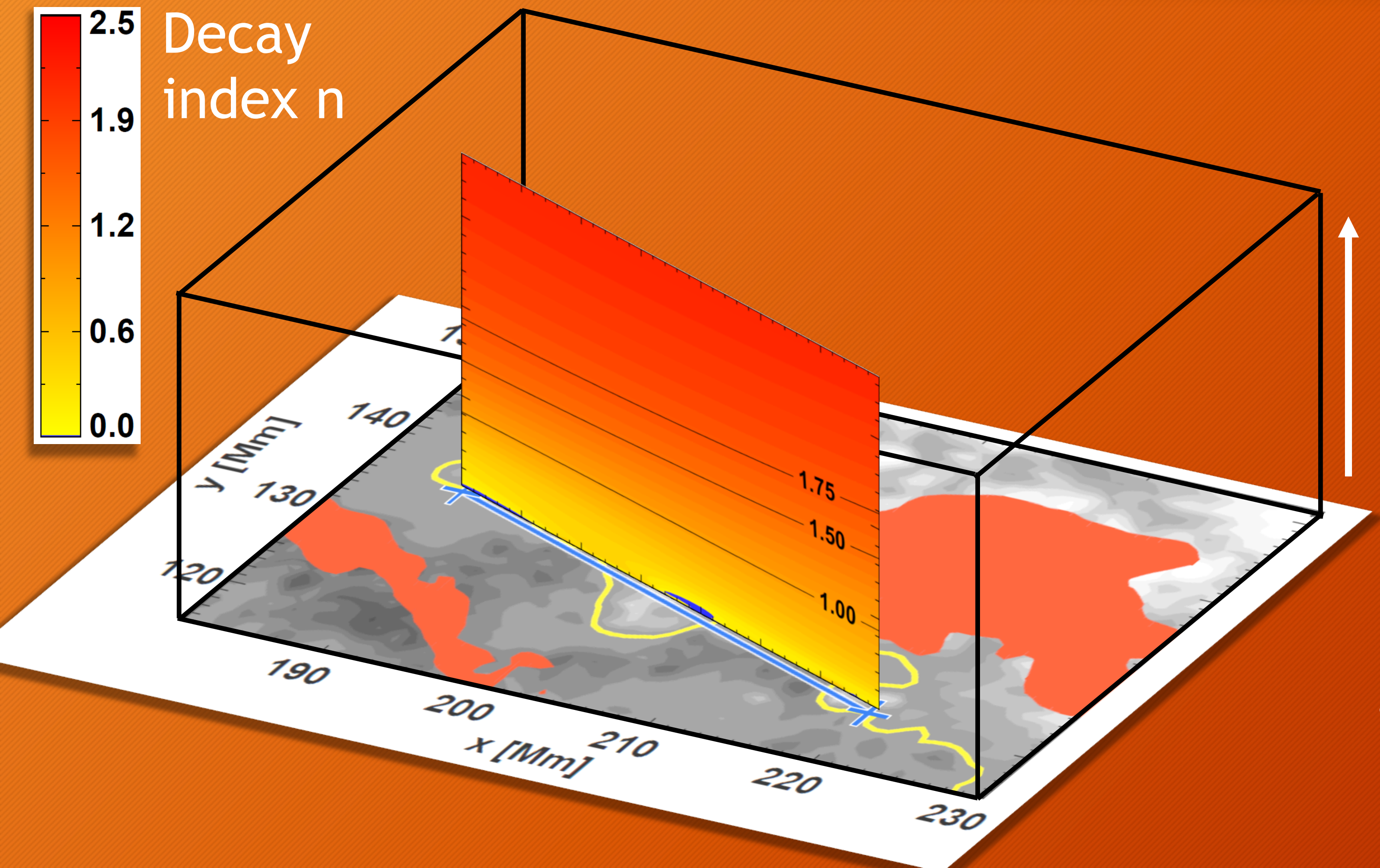


model height above photosphere

Defining a vertical plane above flare-relevant PIL

# Strength of Magnetic Field Above Flare Site

Method

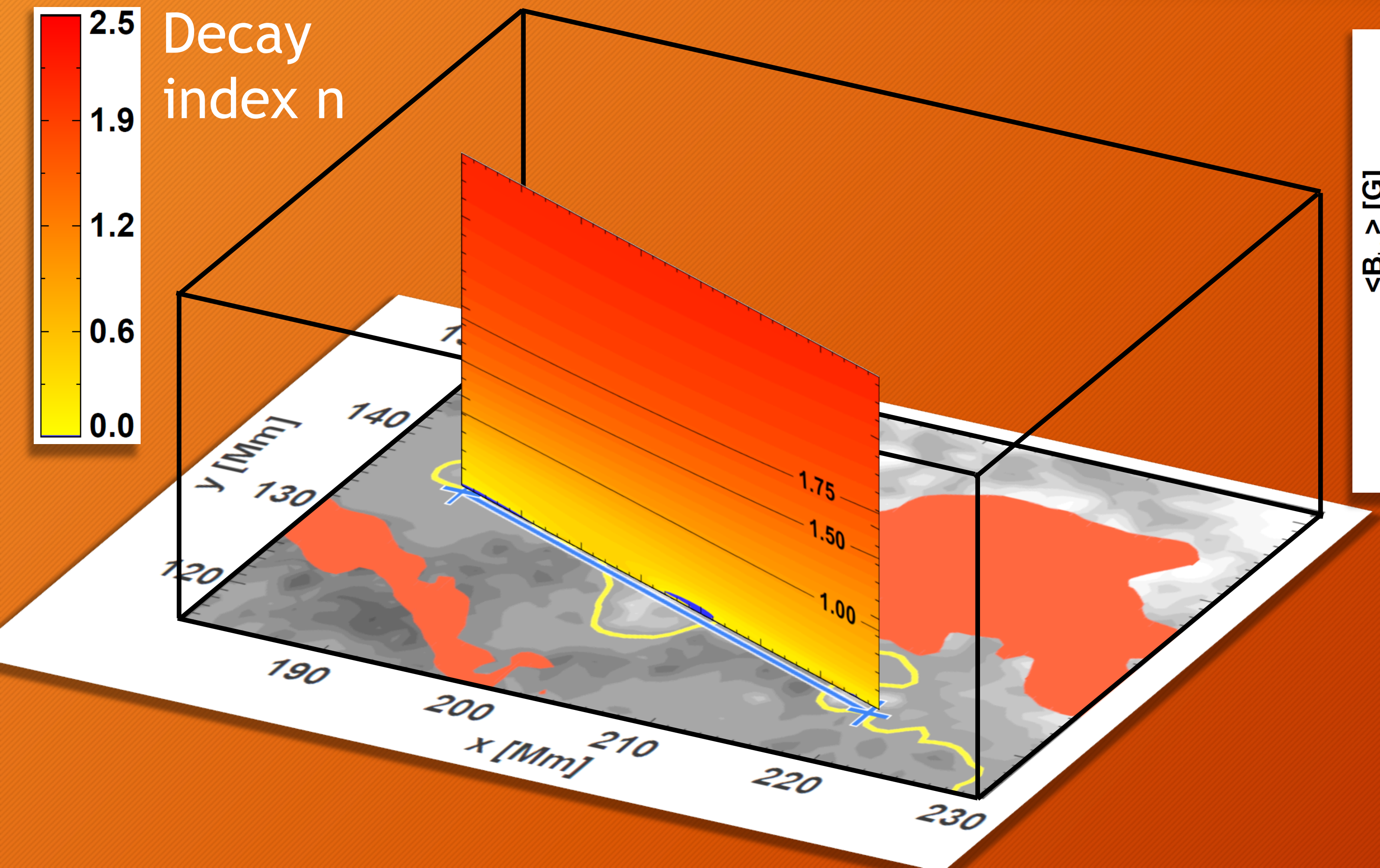


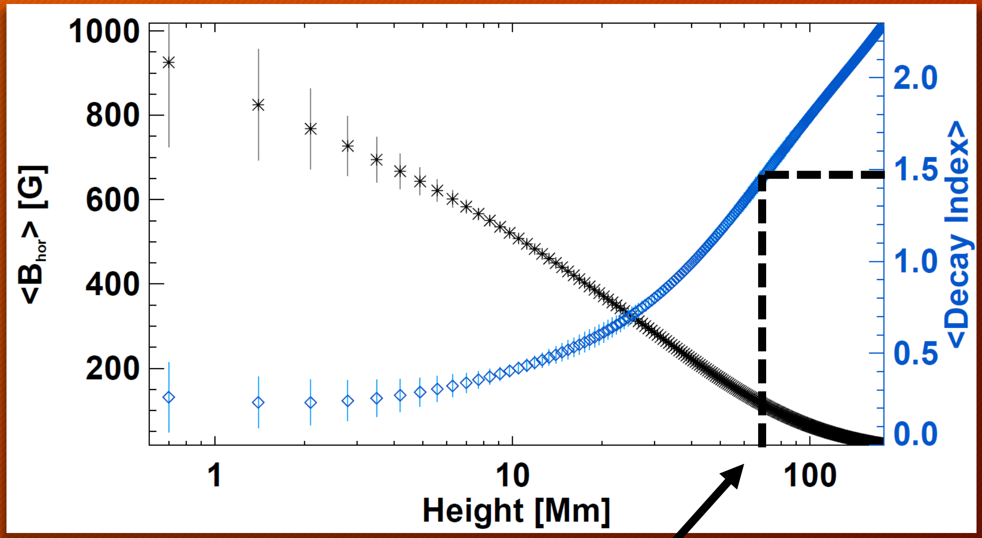


$h_{crit}$ … critical height for torus instability

# Vertical Decay of Magnetic Field above Flare Site

**Results**

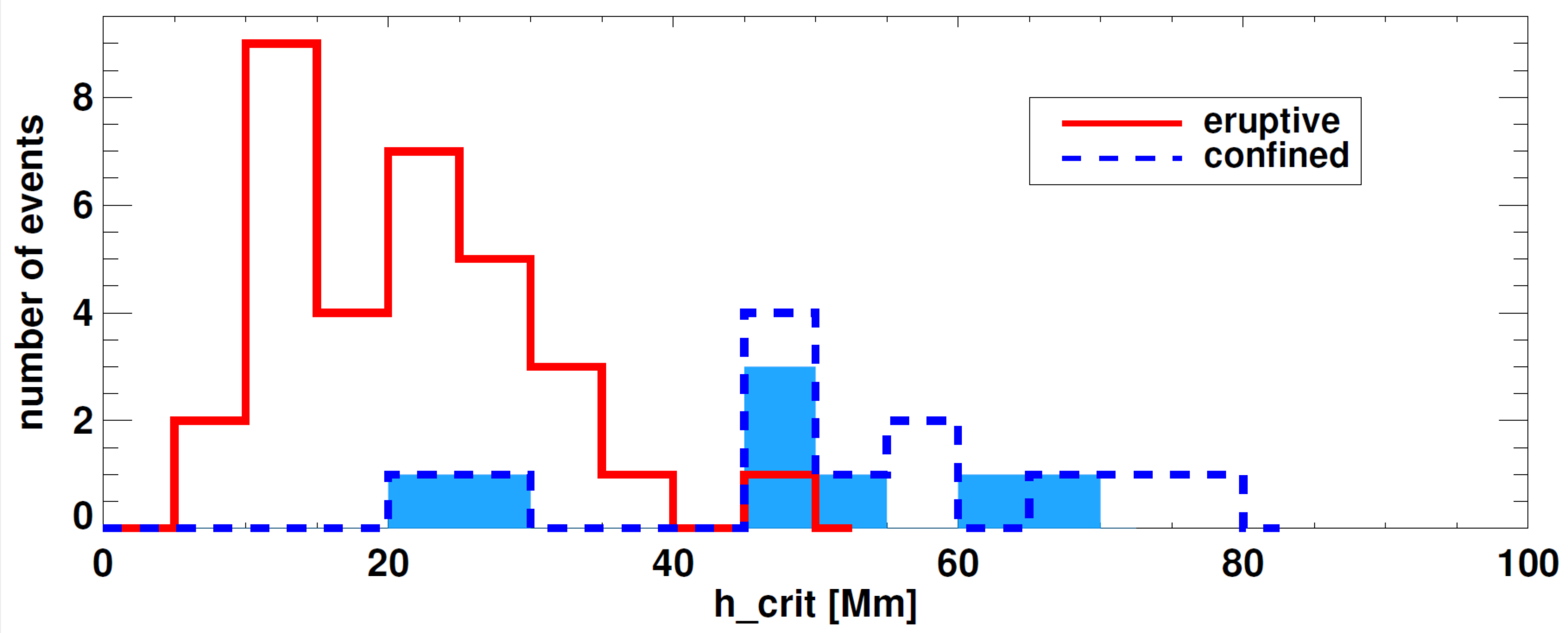


critical height for torus instability

# Orientation of Flare-Relevant Polarity Inversion Line

Method

**PIL … Polarity Inversion Line**

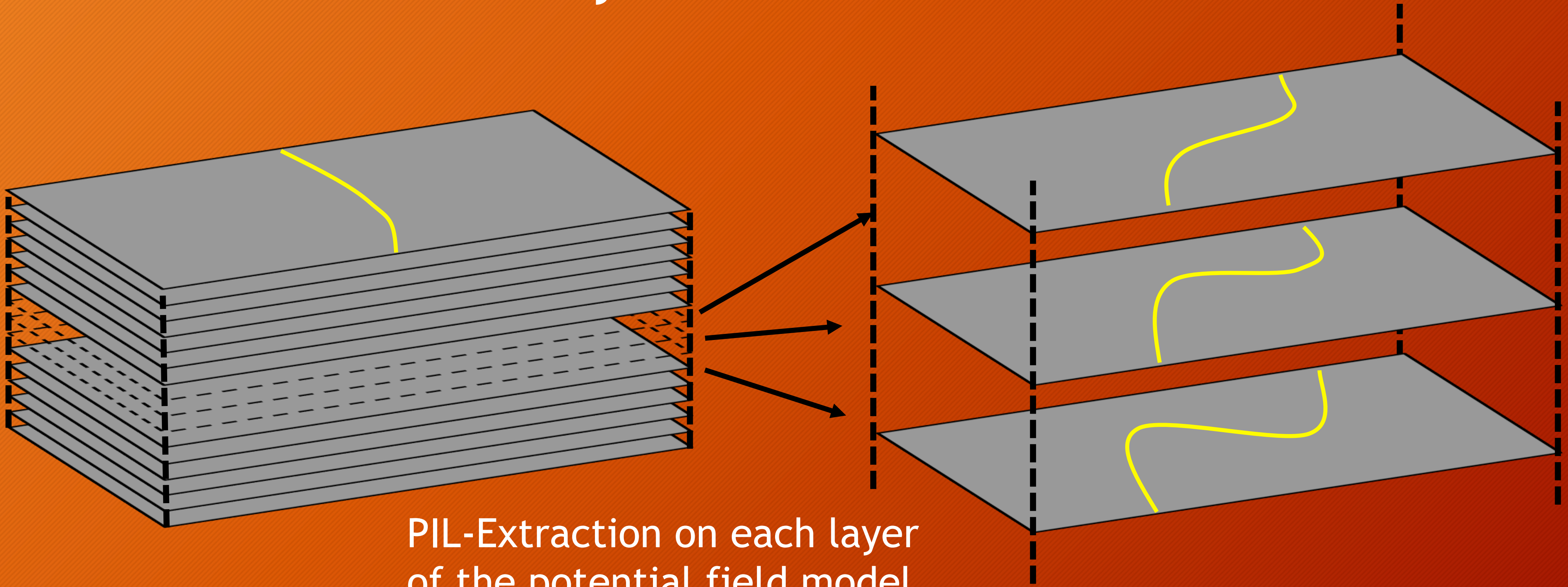

PIL-Extraction on each layer of the potential field model

# Orientation of Flare-Relevant Polarity Inversion Line



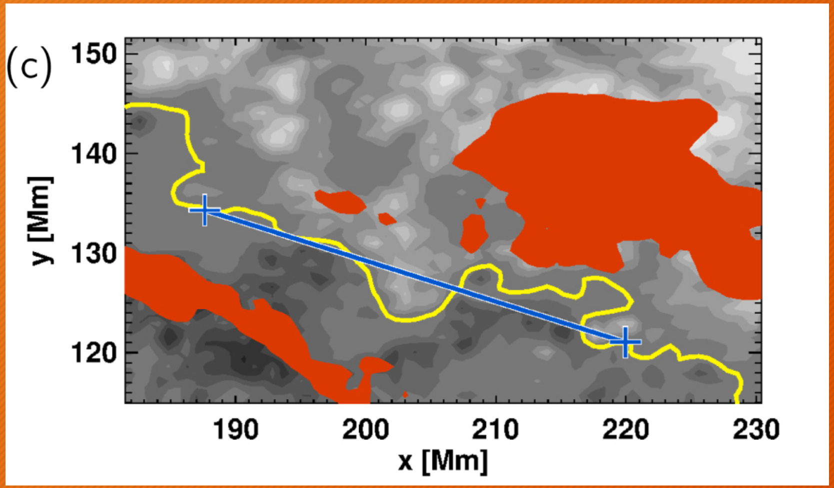


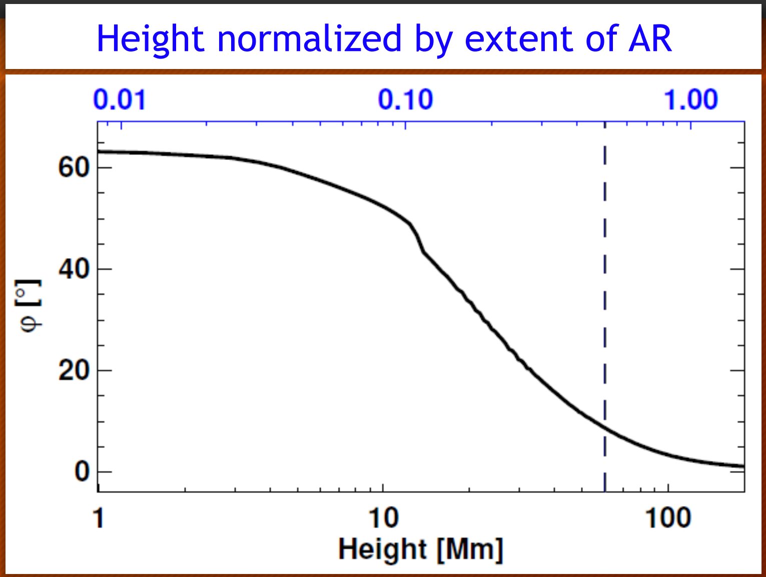


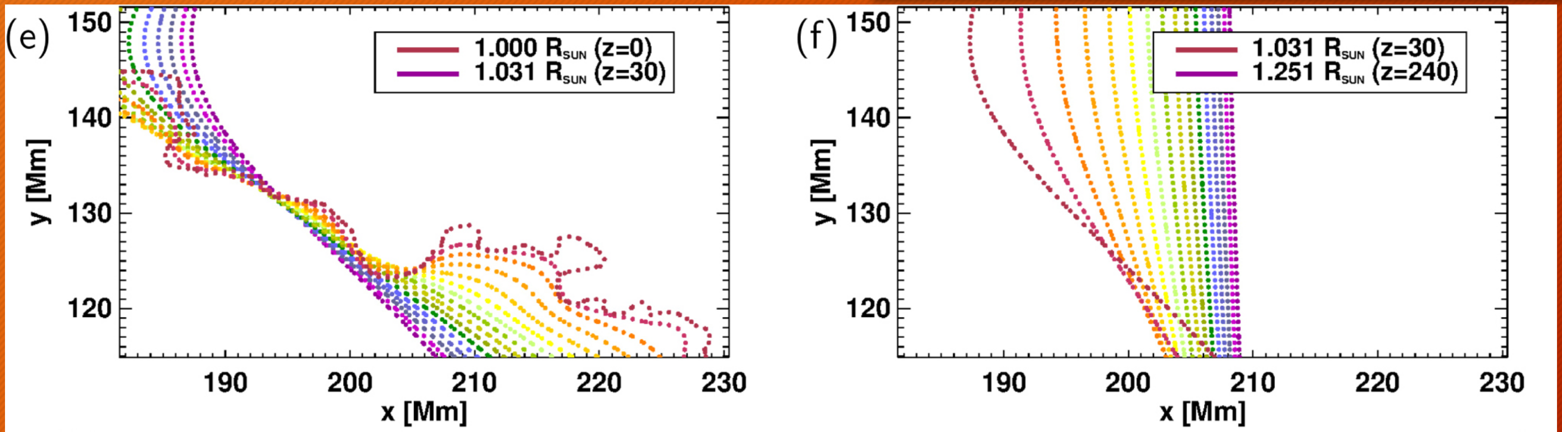

# Orientation of Flare-Relevant Polarity Inversion Line

Results

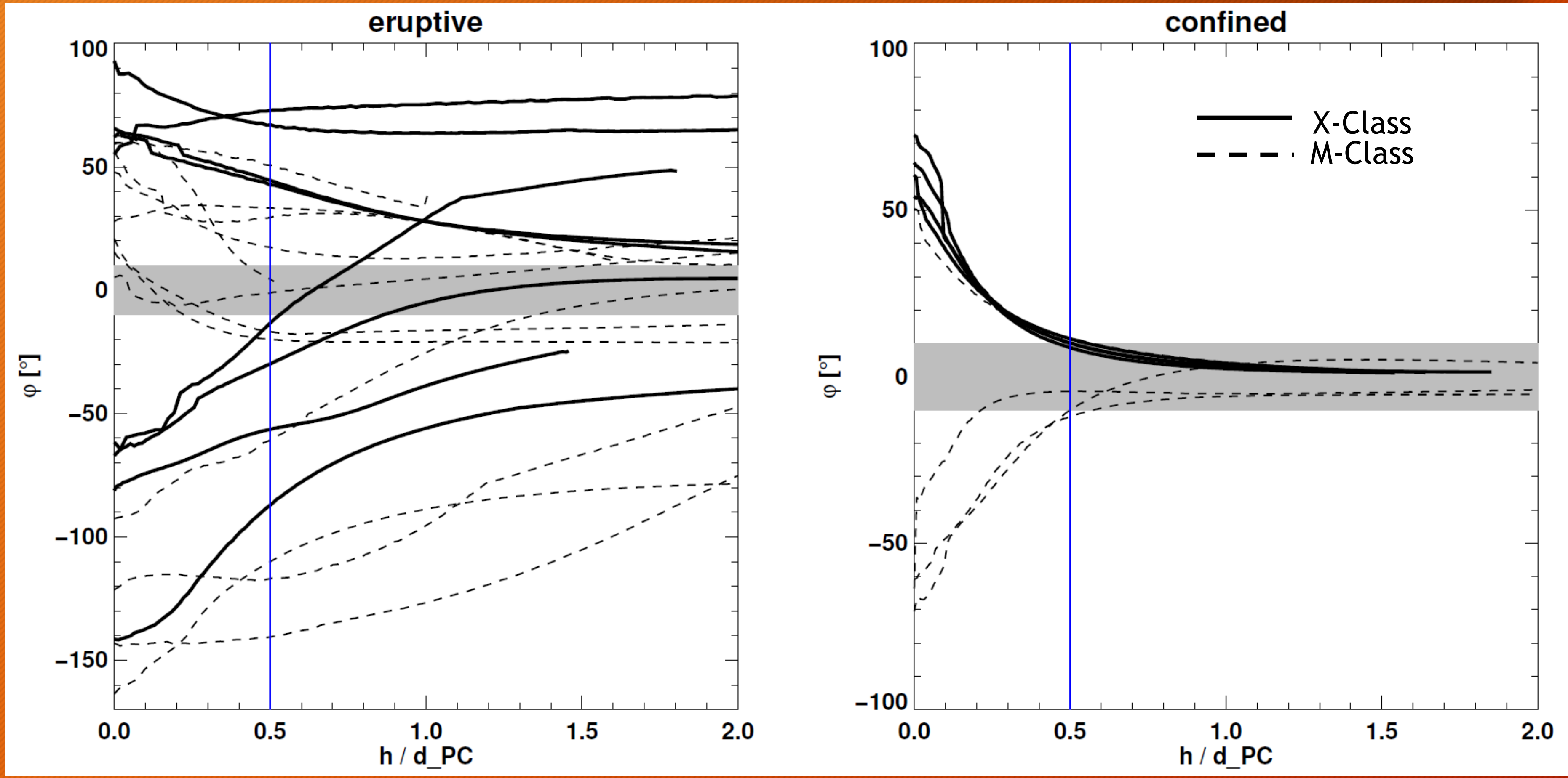


height normalized by the extent of the individual AR dipole ($h/d_{PC}$)

# Orientation of Flare-Relevant Polarity Inversion Line

Results

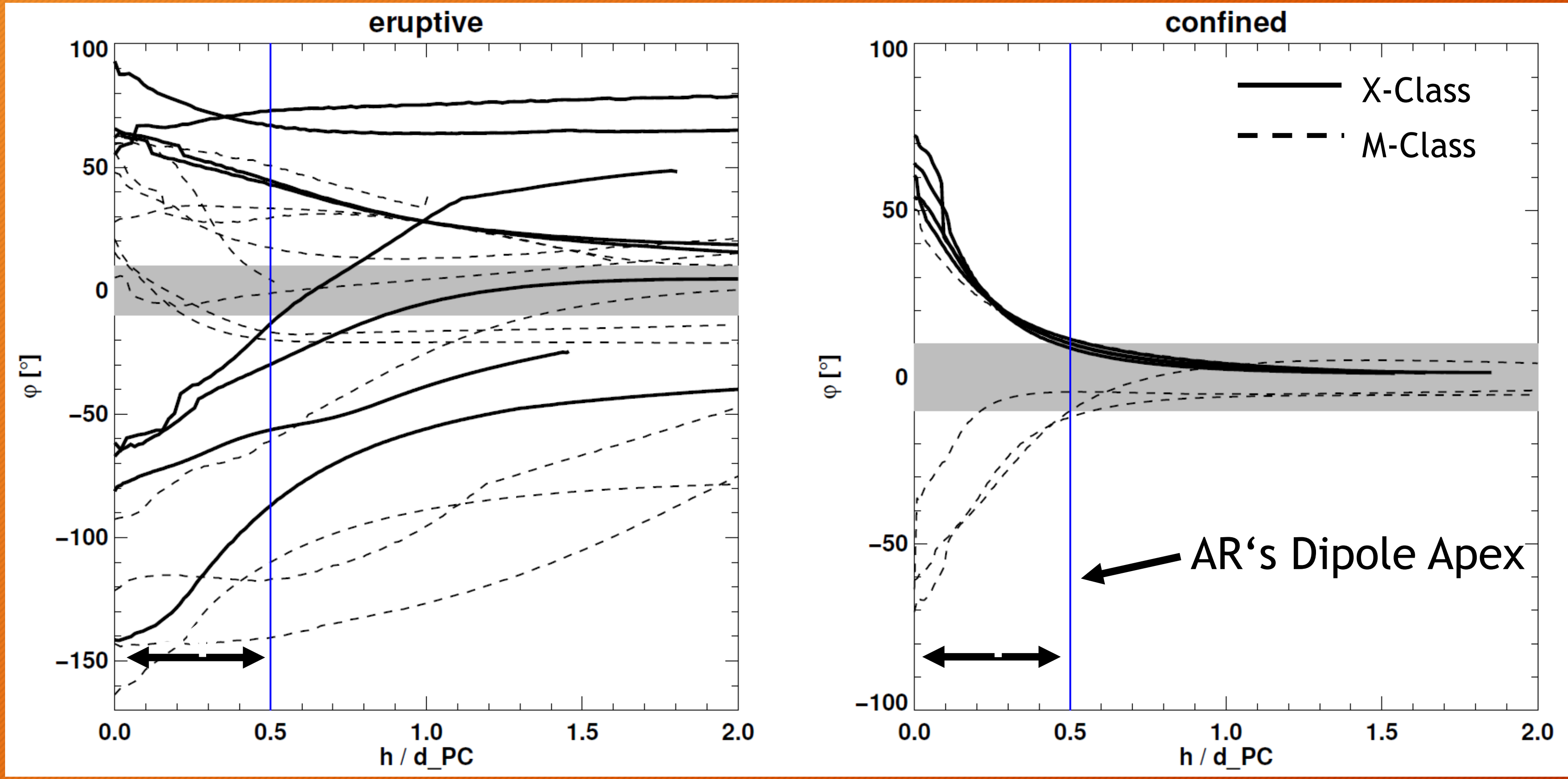


$$\Delta\varphi = |\varphi(h/d_{PC}=0.5) - \varphi(h=0)|$$

Change of orientation of flare-relevant PIL between photosphere and AR dipole apex

height normalized by the extent of the individual AR dipole ($h/d_{PC}$)

# Orientation of Flare-Relevant Polarity Inversion Line

Results

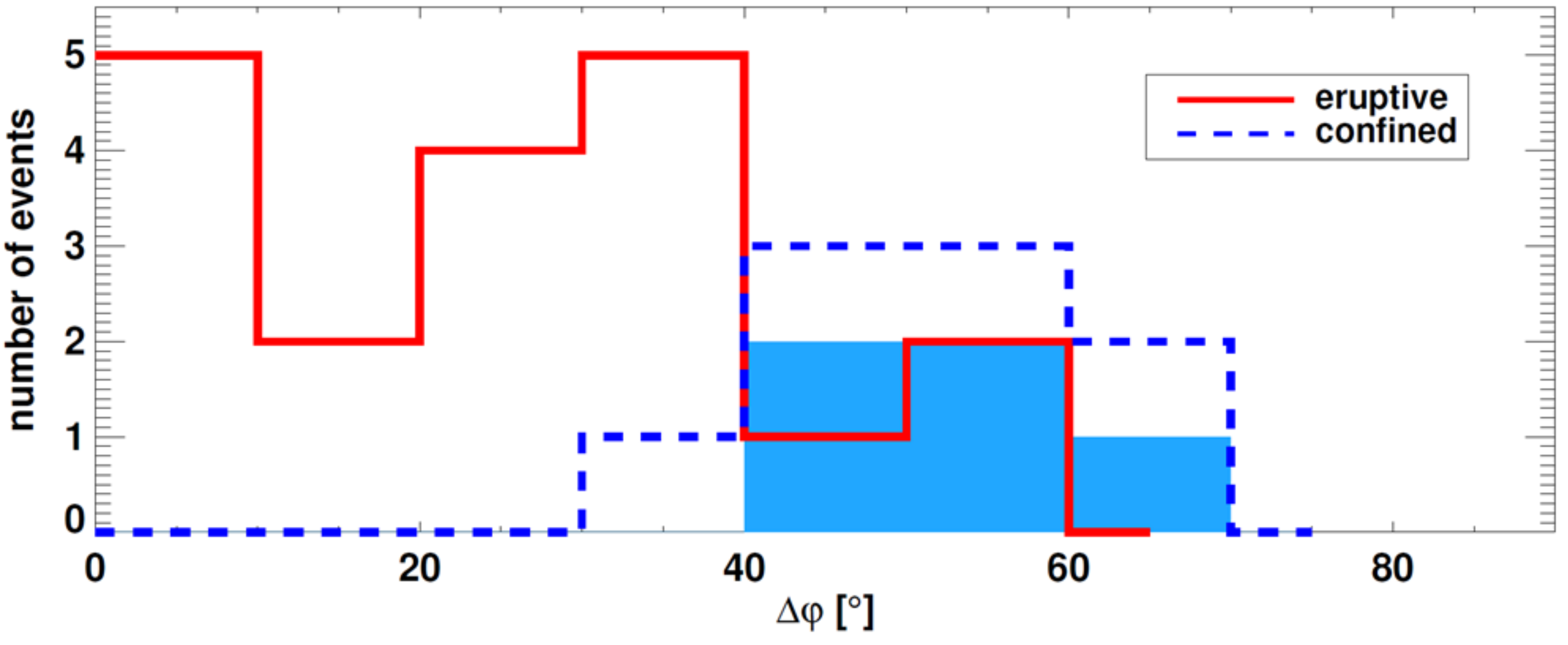


$\Delta\varphi = |\varphi(h/d_{PC}=0.5) - \varphi(h=0)|$

Change of orientation of flare-relevant PIL between photosphere and AR dipole apex

# Orientation of Flare-Relevant Polarity Inversion Line

**Results**

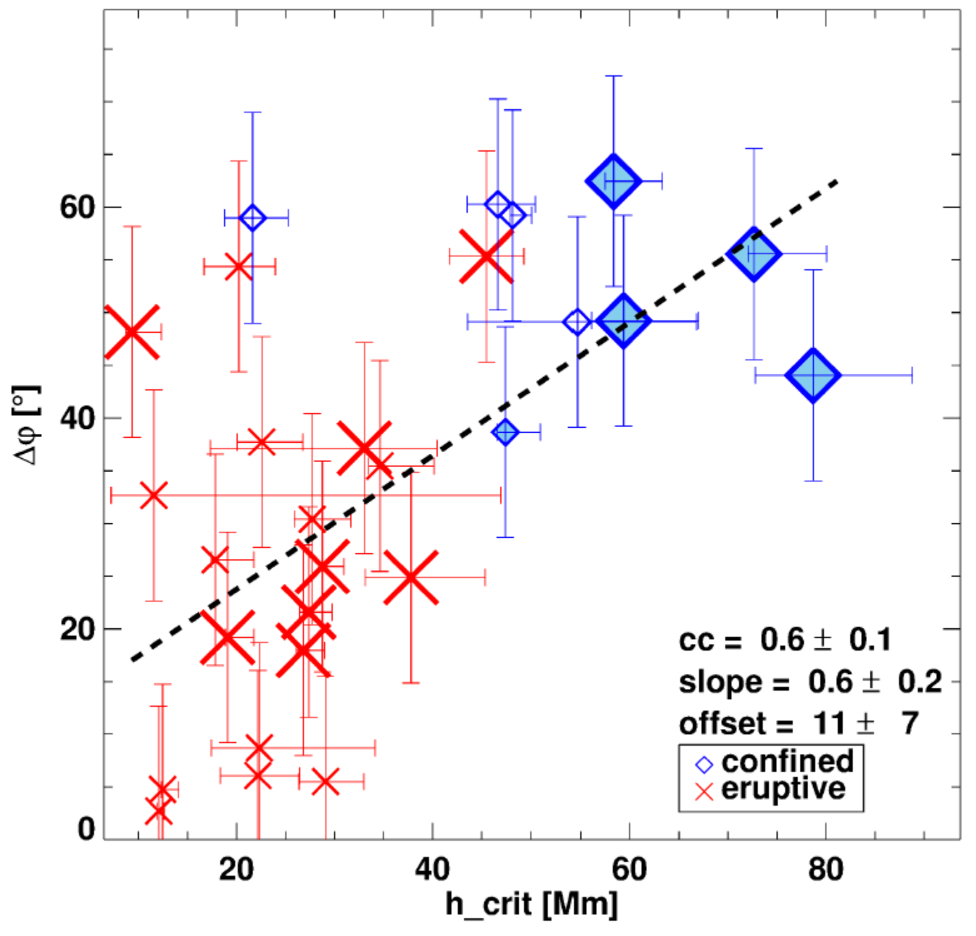


Change of orientation of flare-relevant PIL versus critical height for torus instability

# Summary and Conclusions

Determining factors for large eruptive vs. confined flares are:

- Vertical decay of the host AR magnetic field above flare PIL: in confined flares, magnetic field decays more slowly ($h_{crit}$ is higher)
- Orientation of flare-relevant PIL as function of height:
  confined events → quicker adjustment with respect to global AR field
- Flare location within AR:
  Large flares occurring in AR periphery → tend to be eruptive
  Large confined flares: predominatly located close to AR center, below the „dipole field“ of large ARs (consistent with Wang & Zhang 2007)

Study published in: Baumgartner, Thalmann, Veronig, ApJ 853, 105 (2018)

# Thank you for your attention!

# Orientation of Flare-Relevant Polarity Inversion Line

Results

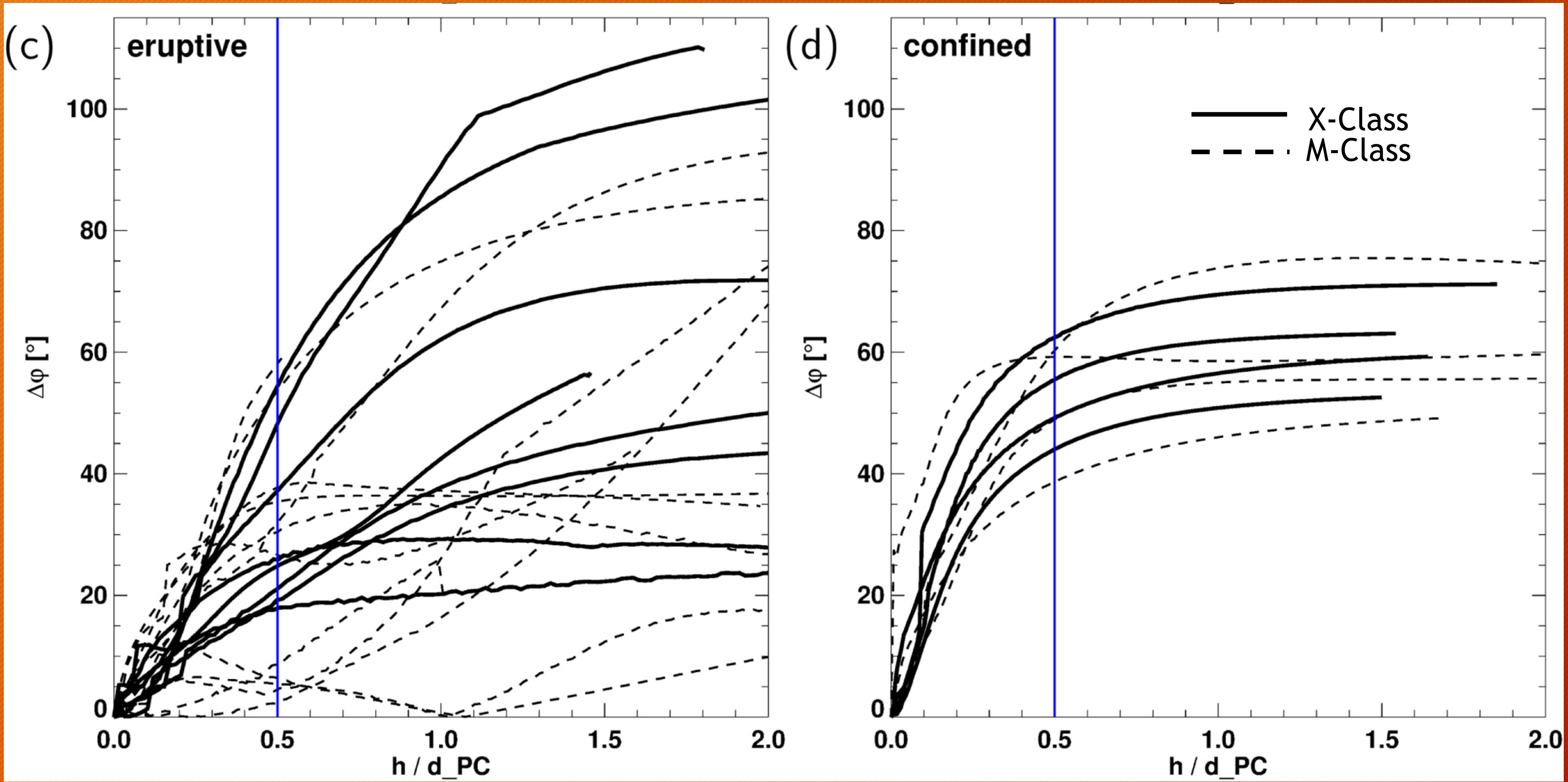


vertical height normalized by the extent of the individual AR dipole ($h/d_{PC}$)

# Bibliography


- C. E. Alissandrakis. On the computation of constant alpha force-free magnetic field. *Astronomy and Astrophysics*, 100:197–200, July 1981.
- C. Baumgartner, J. K. Thalmann, and A. M. Veronig. On the factors determining the eruptive character of solar flares. *Astrophysical Journal*, 853:105, Feb. 2018. doi:10.3847/1538-4357/aaa243
- P. Démoulin and G. Aulanier. Criteria for Flux Rope Eruption: Non-equilibrium Versus Torus Instability. *Astrophysical Journal*, 718:1388–1399, Aug. 2010. doi: 10.1088/0004-637X/718/2/1388.
- Y. Fan and S. E. Gibson. Onset of Coronal Mass Ejections Due to Loss of Confinement of Coronal Flux Ropes. *Astrophysical Journal*, 668:1232–1245, Oct. 2007. doi: 10.1086/521335.
- B. Kliem and T. Török. Torus Instability. *Physical Review Letters*, 96(25):255002, June 2006. doi: 10.1103/PhysRevLett.96.255002.
- J. R. Lemen et al. The Atmospheric Imaging Assembly (AIA) on the Solar Dynamics Observatory (SDO). *Solar Physics*, 275:17–40, Jan. 2012. doi: 10.1007/s11207-011-9776-8.
- J. Schou et al. Design and Ground Calibration of the Helioseismic and Magnetic Imager (HMI) Instrument on the Solar Dynamics Observatory (SDO). *Solar Physics*, 275:229–259, Jan. 2012. doi:10.1007/s11207-011-9842-2.
- T. Török and B. Kliem. Numerical simulations of fast and slow coronal mass ejections. *Astronomische Nachrichten*, 328:743, Oct. 2007. doi: 10.1002/asna.200710795.
- Y. Wang and J. Zhang. A Comparative Study between Eruptive X-Class Flares Associated with Coronal Mass Ejections and Confined X-Class Flares. *Astrophysical Journal*, 665:1428–1438, Aug. 2007. doi: 10.1086/519765.
- F. P. Zuccarello, G. Aulanier, and S. A. Gilchrist. Critical Decay Index at the Onset of Solar Eruptions. *Astrophysical Journal*, 814:126, Dec. 2015. doi: 10.1088/0004-637X/814/2/126.